



**HAL**  
open science

## A Novel Maximum Power Tracking by VSAS approach for Permanent Magnet Direct Drive WECS

B. Meghni, N. M'Sirdi, A. Saadoun, N.K. M'Sirdi

► **To cite this version:**

B. Meghni, N. M'Sirdi, A. Saadoun, N.K. M'Sirdi. A Novel Maximum Power Tracking by VSAS approach for Permanent Magnet Direct Drive WECS. *Energy Procedia*, 2015, 83, pp.79-90. 10.1016/j.egypro.2015.12.198 . hal-01967652

**HAL Id: hal-01967652**

**<https://amu.hal.science/hal-01967652v1>**

Submitted on 1 Jan 2019

**HAL** is a multi-disciplinary open access archive for the deposit and dissemination of scientific research documents, whether they are published or not. The documents may come from teaching and research institutions in France or abroad, or from public or private research centers.

L'archive ouverte pluridisciplinaire **HAL**, est destinée au dépôt et à la diffusion de documents scientifiques de niveau recherche, publiés ou non, émanant des établissements d'enseignement et de recherche français ou étrangers, des laboratoires publics ou privés.



Distributed under a Creative Commons Attribution 4.0 International License

7th International Conference on Sustainability in Energy and Buildings

## A Novel Maximum Power Tracking by VSAS approach for Permanent Magnet Direct Drive WECS

B. Meghni<sup>a</sup>, N.K. M'Sirdi<sup>b</sup>, A. Saadoun<sup>c</sup>

<sup>a</sup>Electrical engineering Department, University of Badji Mokhtar, Annaba 23000, Algeria and laboratory of electromechanical systems research [maghni\\_1990@yahoo.fr](mailto:maghni_1990@yahoo.fr)

<sup>b</sup>Aix Marseille Université, CNRS, ENSAM, Université de Toulon, LSIS UMR 7296 LSIS UMR CNRS UMR, Domaine Universitaire St Jérôme, Avenue Escadrille Normandie-Niemen, 13397 Marseille Cedex 20, France  
[nacer.msirdi@lsis.org](mailto:nacer.msirdi@lsis.org)

<sup>c</sup>Electrical engineering Department, University of Badji Mokhtar, Annaba Algeria and laboratory of electromechanical systems research  
[Abdallahsaadoun555@gmail.com](mailto:Abdallahsaadoun555@gmail.com)

### Abstract

This paper presents control schema of a permanent magnet synchronous generator (PMSG) system with two controllers for generator side and grid side converters in a variable speed wind turbine (VSWT) application. In generator side converter, the most efficient algorithms designed to track the maximum power point (MPP) for catching the maximum wind power is reviewed. For this approach we then design a new maximum power point tracking (MPPT) algorithm using the Variable Structure Automatic Systems approach (VSAS). The proposed approach leads efficient algorithms as shown in this paper by the analysis and simulations. The obtained results show clearly the superiority of the Modified Enhanced Perturb and Observe (MEPO) technique. Using this MPPT method the generated power by the turbine is considered to be, in terms of power control, an auxiliary source feeding a grid. In the grid side converter, active and reactive power control has been achieved by controlling d-axis and q-axis grid current components respectively. The simulation results show the efficiency and reliability of the control strategy proposed in this paper.

© 2015 The Authors. Published by Elsevier Ltd. This is an open access article under the CC BY-NC-ND license

(<http://creativecommons.org/licenses/by-nc-nd/4.0/>).

Peer-review under responsibility of KES International

**Keywords:** PMSG, VSWT, MPPT, VSAS, MEPO;

### 1. Introduction

Over the past ten years, the production of electric energy using wind turbines (WT) has increased due to its cost competitiveness compared to other conventional types of energy resources (petrol and gaz). This production of energy is in full expansion, and different means are now at the dispositions of researchers to finally explore it to the maximum. Variable speed operation and direct drive WT have been the modern aspect of the Wind Energy

Conversion System (WECS) technology, this a type of WT that has been the object of numerous studies over recent years. Variable-speed has many advantages over fixed-speed [1, 2].

In variable speed operation, the WT can be achieved the maximum power operating point for various wind speed by adjusting the rotation speed at optimal value. These characteristics are advantages of variable-speed WECS. In Figure.1, [3] we can see three different operating zones. This paper focuses on the moderate-speed zone (region 2), where the MPPT algorithm is wanted.

Many MPPT techniques have been proposed in [3, 4, 5, 6 and 7]. A lot of them are well established in the literature. They have different aspects and can be classified by: complexity, convergence speed, implementation method, hardware implementation, need for parameterization, sensors required, cost, range of effectiveness, and in other aspects. There are several methods: Tip Speed Ratio method (TSR), optimal torque control method (OTC), and Perturbation and Observation method (P&O), Hill Climbing searching method (HCS), Fuzzy Logic Control method (FLC) and Modified Enhanced (MEPO) among other.

The control system has two controllers for generator side and grid side converters. The first one is to find the best control for catching the maximum wind power. We then recall the most used techniques and then design a new MPPT algorithm using the (VSAS) approach to design a robust and efficient algorithm. This approach has been used successfully for PV Systems and can be applied for WTs as shown in this paper [8]. The task of the second one is to maintain the required DC link voltage level, for this reason, active and reactive power control has been achieved by controlling quadrature and direct current components of grid current respectively. The q-axis current is set at zero for unity power factor and the d-axis current is controlled to deliver the power flowing from the DC-link to the electric utility grid.

The paper is organized as follows. The problem formulation is given in Section 1. Section 2, presents the mathematical models of the different parts of the considered WECS, used for simulation. The models of the WT, the (PMSG) and the converters with connection to the grid are presented. Section 3, presents the most often used MPPT control strategies, for wind turbine driving and then we introduce our new algorithm deduced from the approach considered in [7,8]. After its definition, we compare its results with the widely used MPPT algorithms. In section 4 to achieve smooth regulation of the active and reactive power exchange between the PMSG and the grid, the control of grid side converter is applied. The five section give some simulation results. Finally, a conclusion summarizes the work.

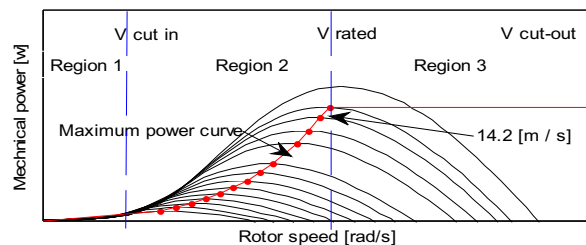


Fig.1.The power characteristic of the considered WT.

## 2. Model of Wind Energy Catching system

In order to ensure extraction of the maximal wind energy, it is necessary to use a power electronic device between the WT generator and the grid, where the frequency is constant, as shown in Fig.2. A WT, a PMSG, AC-DC and DC-AC converters and transformer to be connected to the grid compose the system. All these parts have to be modeled and simulated.

### 2.1. The Wind Turbine model

The input of the WT is the wind and the output is the mechanical power turning the PMSG rotor [9]. For a VSWT, the output mechanical power can be expressed as:

$$P_t = \frac{1}{2} \rho \pi R_t^2 v^3 C_p(\lambda, \beta) \tag{1}$$

The tip speed ratio is given by:

$$\lambda = \frac{R_t \Omega_t}{v} \tag{2}$$

$$P_t = K1 v^3 C_p(\lambda, \beta) , \text{Where } K1 = \frac{1}{2} \rho \pi R_t^2 \tag{3}$$

Where  $P_t$ ( in w) is the output mechanical power available from a wind turbine,  $\rho$  (in  $\text{kg/m}^3$ ) is the air density,  $R_t$  (in meters) is turbine radius,  $v$  (in  $\text{m/s}$ ) is the wind speed,  $C_p$  is the power coefficient,  $\lambda$  is the tip speed ratio,  $\beta$  (in degree) is the blade pitch angle and  $\Omega_t$  (in  $\text{rad/s}$ ) is the rotational speed of the wind turbine shaft.

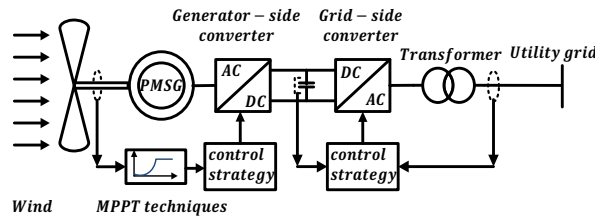


Fig.2. Schematic diagram of the overall system.

According to the manufacturer’s data of the wind turbine and the curve-fitting technique, the power coefficient  $C_p$  can be expressed, with  $\beta$  the adjustable pitch angle of the blade, as [10].

$$C_p = 0.073 \left( \frac{151}{\lambda_i} - 0.058\beta - 0.002\beta^{2.14} - 13.2 \right) e^{-\frac{18.4}{\lambda_i}} ; \text{Where } \lambda_i = \frac{1}{\frac{1}{\lambda - 0.02\beta} - \frac{0.003}{\beta^2 + 1}} \tag{4}$$

By using “Equation (4),” the typical  $C_p$  versus  $\lambda$  curve is shown in Fig.3. In a wind turbine, there is an optimum value of  $\lambda_{opt}$  that leads to  $C_{pmax}$ . When  $\lambda$  in “Equation (2),” is adjusted to its optimal value  $\lambda_{opt}$ , the maximum  $C_p$  is reached when  $\beta = 0$ . The maximum power extraction is achieved. From “Equation (1, 2),” we get:

$$P_{t max} = \frac{1}{2} \rho \pi R_t^5 \left( \frac{C_{p,max}}{\lambda_{opt}^3} \right) \Omega_{t opt}^3 \tag{5}$$

$$\Omega_{t opt} = \frac{\lambda_{opt} v}{R_t} \tag{6}$$

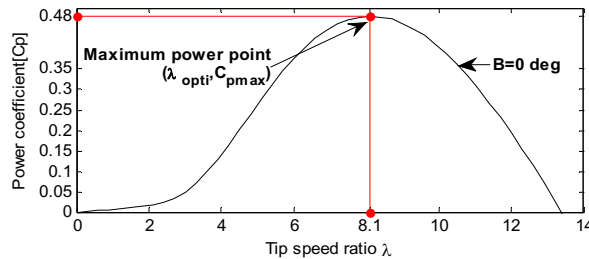


Fig.3. Typical  $C_p$  versus  $\lambda$  curve.

## 2.2. The PMSG model

The PMSG are usually modelled assuming uniform distribution of stator 3-phase windings. So, a simple model of the generator can be obtained by conversion from the three phases reference frame a, b, c to the d, q frame [11, 12].

The model of a three phases PMSG in the d, q reference frame is given by:

$$V_{sd} = R_s I_{sd} + L_d \frac{dI_{sd}}{dt} - \omega_e L_q I_{sq} \quad (7)$$

$$V_{sq} = R_s I_{sq} + L_q \frac{dI_{sq}}{dt} + \omega_e (L_d I_{sd} + \psi_m) \quad (8)$$

Where  $V_{sd}$ ,  $V_{sq}$  (in V) are the direct and quadrature components of the PMSG voltages,  $R_s$ ,  $L_d$  and  $L_q$  represent respectively the stator winding resistance, the direct and the quadrature inductance of the PMSG stator winding,  $\psi_m$  (in wb) represents the magnet flux,  $\omega_e$  (in rad/s) is the electrical rotational speed of PMSG and  $I_{sd}$ ,  $I_{sq}$  (in A) are respectively the direct and quadrature components of the PMSG currents.

Let  $T_e$  (in N.m) be the electromagnetic torque and  $n_p$  be the number of pole pairs. The electromagnetic torque developed by a  $n_p$  machine is given by [11, 12]:

$$T_e = \frac{3}{2} n_p (\psi_m I_{sq} + (L_d - L_q) I_{sd} I_{sq}) \quad (9)$$

## 2.3. The Grid model

The dynamic model of the grid connection, is referred to the rotating frame synchronized with the grid voltage, this allow us to express the model as: [13].

$$V_{dg} = V_{di} - R_g I_{dg} - L_{dg} \frac{dI_{dg}}{dt} + L_{qg} \omega_g I_{qg} \quad (10)$$

$$V_{qg} = V_{qi} - R_g I_{qg} - L_{qg} \frac{dI_{qg}}{dt} - L_{dg} \omega_g I_{dg} \quad (11)$$

Where  $V_{dg}$ ,  $V_{qg}$  (in V) represent the direct and quadrature components of voltages on grid side, while  $V_{di}$ ,  $V_{qi}$  (in V) are the direct and quadrature components of voltages on inverter side, ( $R_g$ ,  $L_{dg}$  and  $L_{qg}$ ) are resistance, the direct and quadrature grid inductance respectively. The direct and quadrature components of the grid currents are  $I_{dg}$ ,  $I_{qg}$  (in A) respectively.

By aligning the d-axis of the reference frame along with the grid voltage position,  $V_{qg} = 0$ , the active and reactive power can be obtained from the following equations:

$$P_g = \frac{3}{2} V_{dg} I_{dg} \quad (12)$$

$$Q_g = \frac{3}{2} V_{dg} I_{qg} \quad (13)$$

Where  $P_g$ ,  $Q_g$  are active and reactive grid powers.

### 3. CONTROL TECHNIQUES

The control system of WECS is divided into two parts; the generator side converter and the grid side converter. These parts allow control of the power delivered to the electrical network and also allow maximum power extraction from wind turbine.

#### 3.1. Control of the generator side converter

The generator side three-phase converter, which is used as a rectifier, works as a driver it controls the rotor speed of the PMSG to achieve variable-speed operation with the (MPPT) control [14]. A cascade control structure with current control loop is employed, as shown in Fig. 4. This control based on PI controller. It's deduced from "Equation (7, 8)," the wind turbine speed can be controlled by regulating the q axis stator current components  $I_{sq}$  the control objective is to track the rotor angular speed. An SVPWM unit is used to produce switching signals based on voltage references.

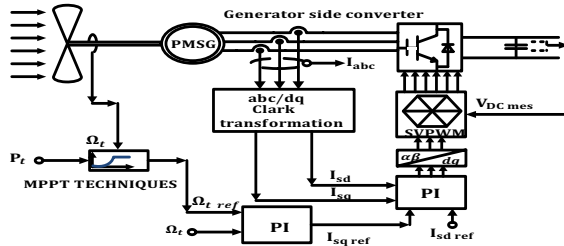


Fig.4. Control block diagram of generator side converter.

#### 3.2. MPPT techniques

The control technique (MPPT) aims to optimize the generator speed in order to maximize the WT output power. Many strategies were investigated to achieve the MPPT. Two control methods are presented (OTC, P&O) and compared to the proposed MEPO algorithm [8]. The power electronic converter may control the turbine rotation speed to get the maximum possible power by means of a MPPT strategy.

##### 3.2.1 The Optimal torque (OT) control

The maximal mechanical torque  $T_{t\max}$ , which is captured by a wind turbine, can be expressed as [15]:

$$T_{t\max} = \frac{1}{2} \rho \pi R_t^5 \left( \frac{C_{p,\max}}{\lambda_{opt}^3} \right) \Omega_{t\,opt}^2 \tag{14}$$

$$T_{t\max} = K_{opt} \Omega_{t\,opt}^2, \text{ Where } K_{opt} = \frac{1}{2} \rho \pi R_t^5 \left( \frac{C_{p,\max}}{\lambda_{opt}^3} \right) \tag{15}$$

The maximum power operation can also be achieved with optimal torque control, the principle of this method is to adjust the PMSG torque according to a maximum power reference torque of the WT at a given wind speed according to the optimal TSR  $\lambda_{opt}$ . The knowledge of  $\lambda_{opt}$  of the turbine is required. Figure.5, shows the block diagram of a WECS with OTC control [16].

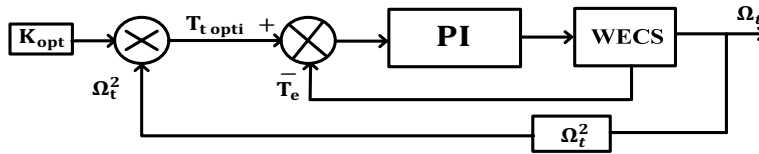


Fig.5.The block diagram of optimal torque control (OTC) MPPT method.

3.2.2 The Perturbation and Observation control (P&O)

The P&O method is one of the simplest MPPT techniques as it involves measurement of the power only. It is based on perturbing the speed  $\Omega_t$  in small step  $d\Omega_t$  and perceiving the resulting changes in turbine mechanical power  $P_t$ , as illustrated by Fig.6, [15, 5]. This algorithm is based on the following procedure: if the operating speed of the WT generator is perturbed in a given direction and if the power supplied by the generator increases, it means that the operating point has moved toward the MPP, and therefore the speed of the machine must still be settled in the same direction (see Fig.7). Otherwise, if power operated generator decreases, the operating point is far from the MPP and therefore the direction of the disturbance in the speed of operation must be reversed see eg [12, 13].

Additionally, selecting an appropriate step size is not a simple task: though larger step-size means a faster response and more oscillations around the peak point, and hence, less efficiency, a smaller step-size improves efficiency but decreases the convergence speed [5, 17] as represented in Fig.7 and compared to the MEPO and the OTC methods.

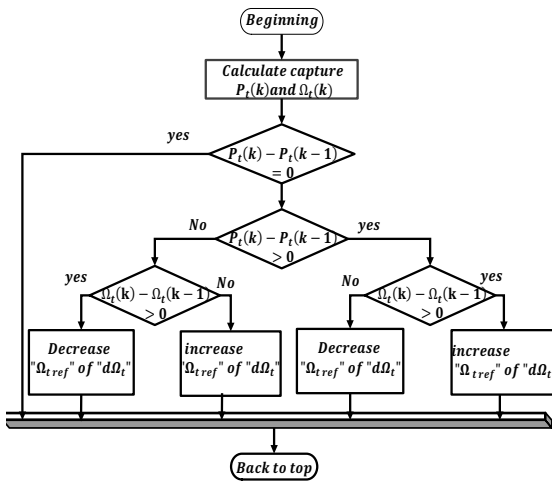


Fig.6.Flowchart of the (P&O.) MPPT method.

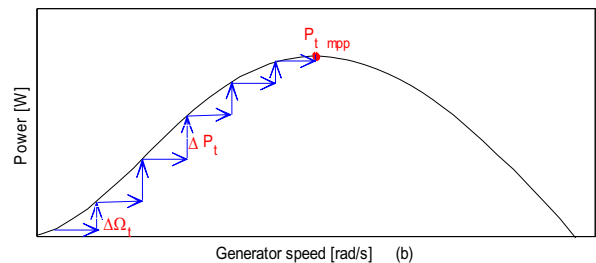
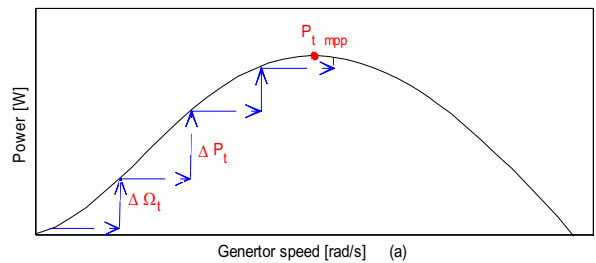


Fig.7. Size of  $\Delta\Omega_t$ , (a) a larger step-size; (b) a smaller step-size.

3.2.3 The Modified Enhanced P&O Algorithm (MEPO)

For fast and very good converging algorithms, the Operation Point moves essentially on a wind dependant characteristic. The change of wind velocity forces it to change from one characteristic curve to another, generally more or less near the new optimum. The maximum Power depends on the WT rotation speed  $\Omega_t$  and time:  $P_t(t) = P_t(\Omega_t(t))$ .

Then the required Maximum Power Point to Track is really defined by the following objective function:

$$\frac{dP_t(t)}{dt} = 0 \text{ or } \frac{dP_t(t)}{dt} = \frac{dP_t}{d\Omega_t} \cdot \frac{d\Omega_t}{dt} = 0 \quad (16)$$

We can define as Lyapunov function the positive function  $W(t)$  where we use a positive constant  $P_0 > P_t$  greater than the maximum power which can be got by the WT.  $W(t)$  is always positive.

$$W(t) = (P_0 - P_t(t))^2 > 0 \quad (17)$$

Its time derivative  $\frac{dW(t)}{dt}$  must be negative to make  $W(t)$  always decreasing and then convergence of the algorithm.

$$\frac{dW(t)}{dt} = -\frac{dP_t(t)}{dt} (P_0 - P_t(t)) < 0 \quad (18)$$

Then, to verify this condition,  $\frac{dP_t(t)}{dt} > 0$  must be positive. Let us now consider the control in case of discrete time, like do all the above-presented algorithms. We can estimate the Power derivative  $\frac{dP_t(t)}{dt} = \frac{dP_t}{d\Omega_t} \cdot \frac{d\Omega_t}{dt}$  by:

$$(P(\Omega_t + \Delta\Omega_t) - P(\Omega_t)) \cdot \Delta\Omega_t = \Delta P \cdot \Delta\Omega_t > 0 \quad (19)$$

Then we choose for the rotational speed perturbation  $\Delta\Omega_t = K \cdot \text{sign}(\Delta P \cdot \Delta\Omega_t)$

The fetched MPPT may be defined, in the MEPO algorithm by the following:  $\Delta\Omega_t = K \text{sign}(\Delta P \cdot \Delta\Omega_t)$

In case of no change in the output power after perturbation:  $\Delta P_t(k) = 0$ , then as

In case of  $\Delta P_t(k) \geq 0$ , the power increase after positive perturbation delta w then let us continue in the same direction .

In case of  $\Delta P_t(k) \leq 0$ , the power decreases after positive perturbation delta w then let us continue in the reverse direction .Finally for the rotation speed control we get the following control law:

$$\Omega_{tref} = \Omega_t + K \text{sign}(\Delta P \cdot \Delta\Omega_t), \text{ with } k = 1 \quad (20)$$

### 3.3. Control of the grid side converter

The main of grid side converter (GSC) maintains the DC bus voltage stable and also controls the reactive power exchange between the PMSG and the grid, i.e., the main GSC transfers the active power extracted from the wind turbine to the grid at an adjustable power factor to the grid during wind variation or load transients [18]. Figure .8, shows the control diagram for the main GSC implemented in synchronous rotating dq reference; the outer loop contains a DC link voltage control, which produces the currents reference  $I_{dg\text{ref}}$  for the active power controller. The inner loop contains the currents  $I_{dg}$ ,  $I_{qg}$  controlled by the PI controller.



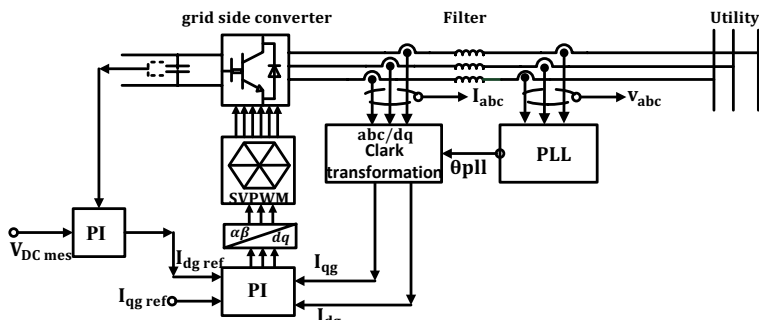


Fig.8. Control block diagram of grid side converter.

**4. Simulation results and Discussion**

The simulation has been carried out using Matlab Simulink package, under a wind speed profile whose mean value is (11.5 m/s). The evaluation tests have been done with the wind speed input defined by Fig.9, got from a Matlab Simulation. The system parameters are given in the appendix A.

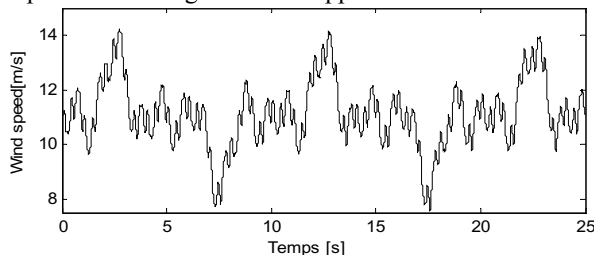


Fig.9. Wind speed variation in (m/s).

The  $C_p$  and the output power is shown in the following for each one of the presented algorithms. The studied and proposed algorithm MEPO based on VSAS approach is tested in simulation and compared with the different MPPT methods (OTC, P&O) are shown in Figs (10, 11 ,12 and 13); The simulation results are summarized in Table I [2].

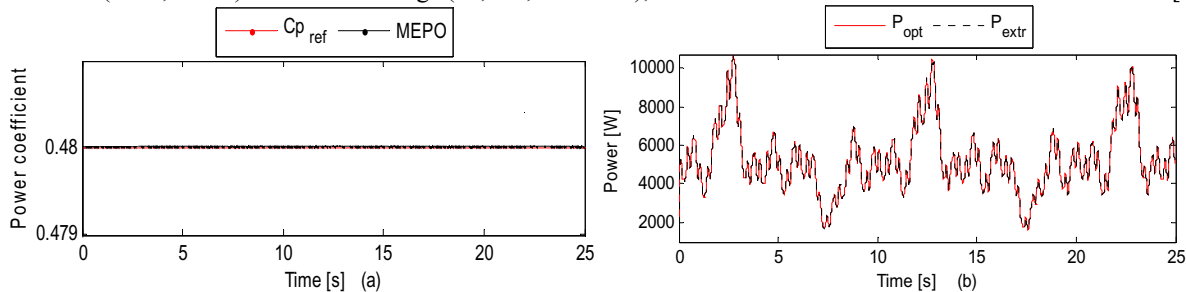


Fig.10. (a)  $C_p$  ; (b) optimal and extracted power For [MEPO MPPT].

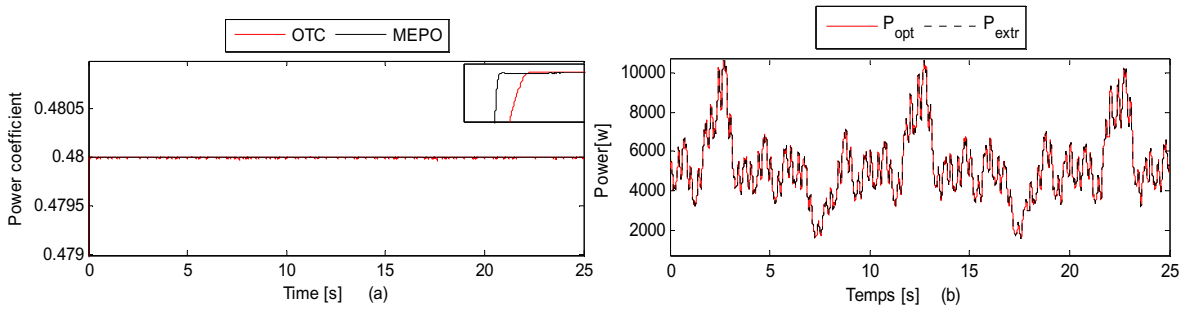


Fig.11. (a)  $C_p$  ; (b)optimal and extracted power For [OTC MPPT].

The MPPT controller ensures the tracking of the optimum power points at variable wind speeds, by maintaining the power coefficient to its maximum value  $C_{p\ max} = 0.48$  as shown in Fig.10 (a). Based on the results demonstrated in Figs (11(a), 12 (a), 13(a))the MEPO method were found to be the fastest to reach the steady-state, This shows the effectiveness of the proposed algorithms. While the other algorithms exhibiting a slight difference. In contrast with MEPO, the classical P & O for ( $x=5$ ) and OTC method of are very slow.

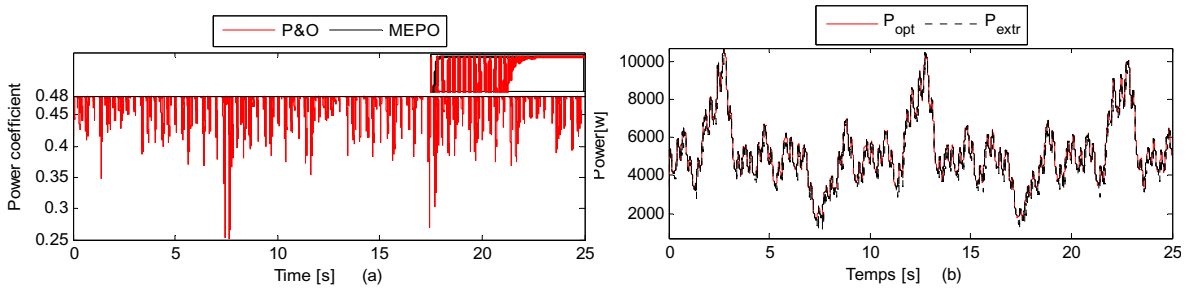


Fig.12. (a)  $C_p$ ; (b)optimal and extracted power For [P&O MPPT , $x=5$ ].

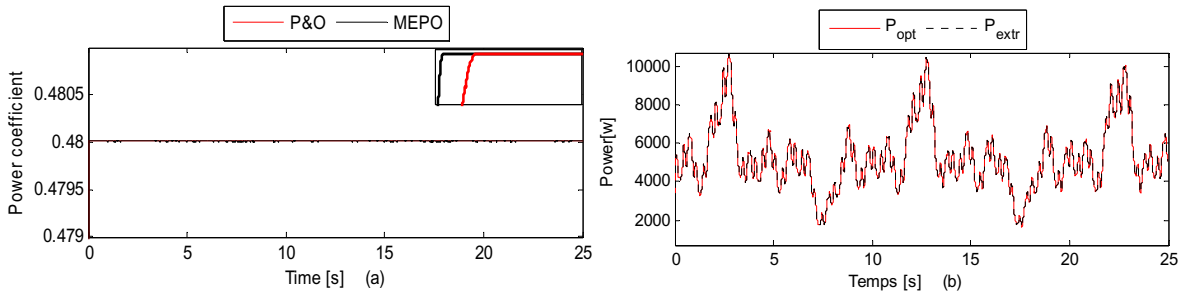


Fig.13. (a)  $C_p$  ; (b)optimal and extracted power For [P&O MPPT , $x=0.1$ ].

The control algorithm based on MEPO and OTC achieves the highest average value of  $C_{p\ max}$  to an approximate value of 0.480. By comparison, the P&O for ( $x=0.1$ ) gives an average value of  $C_{p\ max} = 0.4792$ . Since the average value of  $C_{p\ max}$  of the classical P&O for ( $x=5$ ) method is 0.4780, this method is the least effective.

The verification of maximum power tracking control is illustrated in Figs (10(b), 11(b), 12 (b) and 13(b)).The wind speed profiles of maximum power tracking control  $P_{opt}$  is also shown in Figs (10(b), 11(b), 12 (b) and 13(b)).From the figures, it has been found that, in the four methods (OTC, P&O,MEPO), the extracted power by the turbine follow the desired trajectory  $P_{opt}$  with different efficiency; the calculated efficiencies are listed in Table I.

Table 1 .Summary of performance of four algorithms

MPPT technique	Average power Pt ( kw)	Losing power Pt ( w)	Power coefficient	Tip speed ratio	Response time ( s)	Efficiency (Pt/Popt) %
OTC	2.2624	0.0311	0.4798	8.0990	0.030	$\cong 100$
P&O X=0.1	2.2598	0.1982	0.4792	8.0983	0.215	99.97
P&O X=5	2.2463	7.4252	0.4780	8.1233	0.0405	99.57
<b>MEPO</b>	<b>2.2613</b>	<b>0.0877</b>	<b>0.4800</b>	<b>8.0992</b>	<b>0.01</b>	$\cong 100$

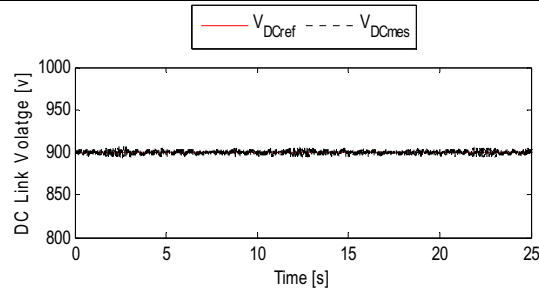


Fig.14. DC Link Voltage (v).

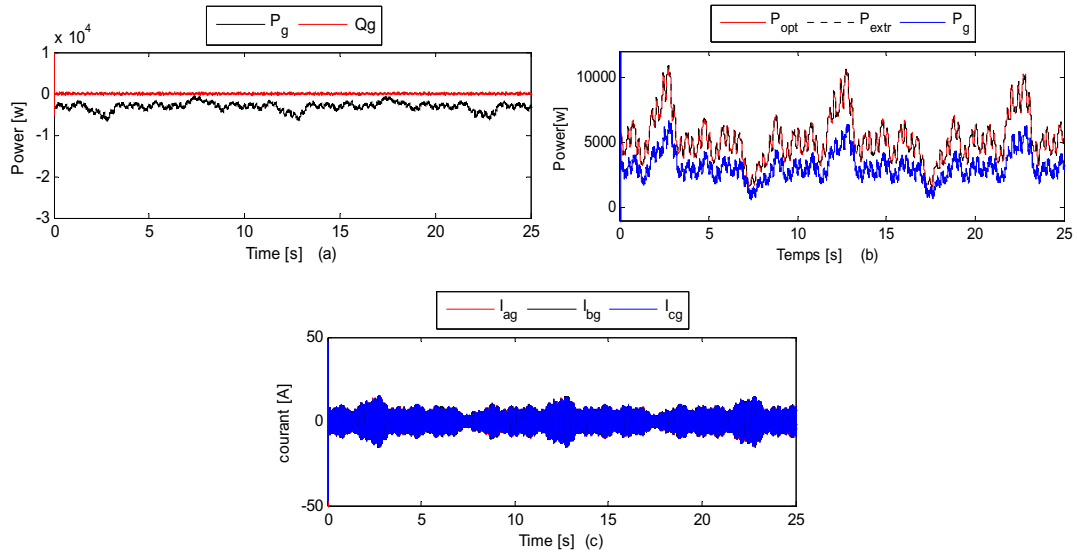


Fig.15. (a) active and reactive power ;(b) extracted and delivered grid power ;(c)Grid currents (A).

In the control of grid side converter, the DC bus voltage is represented in Fig.14, which demonstrates that this voltage is perfectly constant equal to 900 V and thus proved the effectiveness of the outer loop control applied in this part. In the inner loop control, Fig.15 (a, b), shows the active power of grid which is substantially equal, except for the losses, to the extracted power by wind source. It can be seen that, with the change of (wind speed, optimal power and extracted power), active grid power is adjusted and tracking with the change of the wind speed. The reactive power reference value is maintained equal to zero demonstrated in Fig.15 (a) then we operate with unitary power factor. The injected currents to the grid are represented in Fig .16.

## 5. Conclusion

The PMSG is nowadays a popular choice for wind energy conversion systems. This popularity is mostly due to its ability for large variable speed drive. In this paper we present the models of the different parts of a WECS: the generator side and the grid side converters have been modeled in Simulink. The generator side controller has been used to track the maximum power generated from WT. In this part, OTC and classical P&O methods MPPT are reviewed and discussed, for wind turbine driving and we propose a new MPPT algorithm (MEPO) deduced from the VSAS approach. We analyze a simulation and comparison of three selected control methods in terms of efficiency and speed of response.

The verification of maximum power tracking control is illustrated in the presented figures show that the best MPPT algorithm is the MEPO. The wind speed profiles of maximum power tracking control  $P_{opt}$  and the dynamic difference between the turbine powers  $P_t$  is also shown. From the figures, it has been found that, in the four methods (MEPO, OTC, P&O), the extracted power by the turbine follow the desired trajectory  $P_{opt}$  with different efficiency; the calculated efficiencies are listed in Table I.

In the grid side converter, active and reactive power control has been achieved by controlling d-axis and q-axis grid current components respectively. The q-axis grid current is controlled to be zero for unity power factor and the d-axis grid current is controlled to deliver the power flowing from the DC-link to the grid.

The simulation results involve the complete model of the system and prove the superiority of MEPO MPPT method and the whole control system.

## Appendix A.

Table 2. Wind turbine Parameters

Radius of the turbine	$R_t = 2$ m
Volume density of the air	$\rho = 1.225$ kg. m <sup>3</sup>
The pitch angle	$\beta = 0^\circ$
specific optimal speed	$\lambda_{opti} = 8.1$
Coefficient of maximum power	$C_{p\ max} = 0.48$

Table 3. PMSG parameters

Rated power	$P = 10$ kw
Stator resistance	$R_s = 0.00829\Omega$
Direct stator inductance	$L_d = 0.174$ mH
Stator inductance quadrature	$L_q = 0.174$ mH
Field flux	$\psi_f = 0.071$ wb
Number of pole pairs	$n_p = 6$ paire pole

## References

- [1] Oghafy, V., & Nikkhajoei, H. (2008, July). Maximum power extraction for a wind-turbine generator with no wind speed sensor. In Power and Energy Society General Meeting-Conversion and Delivery of Electrical Energy in the 21st Century, 2008 IEEE (pp. 1-6). IEEE.
- [2] Abdullah M A, Yatim A H M, Tan C W, et al. A review of maximum power point tracking algorithms for wind energy systems. *Renewable and Sustainable Energy Reviews*. 2012; vol. 16, no 5, p. 3220-3227.
- [3] Raza Kazmi S M, Goto Hiroki, Guo Hai-Jiao, et al. Review and critical analysis of the research papers published till date on maximum power point tracking in wind energy conversion system. In: *Energy Conversion Congress and Exposition (ECCE)*. IEEE 2010; p. 4075-4082.
- [4] Hui Joanne, Bakhshai Alireza. A new adaptive control algorithm for maximum power point tracking for wind energy conversion systems. In: *Power Electronics Specialists Conference(PESC)*. IEEE 2008; p. 4003-4007.
- [5] Raza Kazmi S M, Goto Hiroki, Guo Hai-Jiao, et al. A novel algorithm for fast and efficient speed-sensorless maximum power point tracking in wind energy conversion systems. *Industrial Electronics*. IEEE Transactions on. 2011; vol. 58, no 1, p. 29-36.
- [6] Musunuri Shravana, GINN H L. Comprehensive review of wind energy maximum power extraction algorithms. In: *Power and Energy Society General Meeting*. IEEE, 2011; p. 1-8.
- [7] N K. M'Sirdi, B. Nehme, M. Abarkan, A. Rabhi. The Best MPPT Algorithms by VSAS approach for Renewable Energy Sources (RES) . *Int. Conference EFEA 2014*, Paris, Nov 2014.
- [8] M'Sirdi, N. K., Rabhi, A., & Abarkan, M. (2013). A New VSAS approach for Maximum Power Tracking for Renewable Energy Sources (RES). *Energy Procedia*, 42, 708-717.
- [9] Tan Kelvin, Islam Syed. Optimum control strategies in energy conversion of PMSG wind turbine system without mechanical sensors. *Energy Conversion*. IEEE Transactions on. 2004; vol. 19, no 2, p. 392-399.

- [10] LIN, Whei-Min et HONG, Chih-Ming. Intelligent approach to maximum power point tracking control strategy for variable-speed wind turbine generation system. *Energy*, 2010, vol. 35, no 6, p. 2440-2447.
- [11] Munteanu Iulian, Bratcu Antoneta Iuliana, Cutululis Nicolaos-Antonio, et al. *Optimal control of wind energy systems: towards a global approach*. Springer. 2008.
- [12] YIN Ming, LI Gengyin, Zhou Ming, Et Al. Modeling of the wind turbine with a permanent magnet synchronous generator for integration. In: *Power Engineering Society General Meeting*. IEEE.2007; p. 1-6.
- [13] Chinchilla Monica, Arnaltes Santiago, Et Burgos Juan Carlos. Control of permanent-magnet generators applied to variable-speed wind energy systems connected to the grid. *Energy Conversion*. IEEE Transactions on.2006; vol. 21, no 1, p. 130-135.
- [14] Massoum A, Fellah M-K, Meroufe A. Sliding mode control for a permanent magnet synchronous machine fed by three levels inverter using a singular perturbation decoupling. *Journal Of Electrical & Electronics Engineering*. Vol 5. Istanbul university – 2005
- [15] Koutroulis Eftichios , Kalaitzakis Kostas. Design of a maximum power tracking system for wind-energy-conversion applications. *Industrial Electronics*. IEEE Transactions on. 2006; vol. 53, no 2, p. 486-494.
- [16] Shirazi M, Viki AH, Babayi O. A comparative study of maximum power extraction strategies in PMSG wind turbine system. In: *2009 IEEE Electrical Power & Energy Conference (EPEC)*. 2009. p. 1–6.
- [17] Pan Ching-Tsai, Juan Yu-Ling. A novel sensorless MPPT controller for a high-efficiency microscale wind power generation system. *Energy Conversion*. IEEE Transactions on. 2010; vol. 25, no 1, p. 207-216.
- [18] Daoud Ahmed A, Dessouky Sobhy S, Salem Ahmed A. Control scheme of PMSG based wind turbine for utility network connection. *IEEE Proc* 2011. 978-14244-8782-0/11.